

Ab initio Pseudopotential Plane-wave Calculations of the Electronic Structure of $\text{YBa}_2\text{Cu}_3\text{O}_7$

Hanchul Kim and Jisoon Ihm

Department of Physics and Center for Theoretical Physics,

Seoul National University, Seoul, 151-742, Korea

(September 15, 1994)

Abstract

We present an *ab initio* pseudopotential local density functional calculation for stoichiometric high- T_c cuprate $\text{YBa}_2\text{Cu}_3\text{O}_7$ using the plane-wave basis set. We have overcome well-known difficulties in applying pseudopotential methods to first-row elements, transition metals, and rare-earth materials by carefully generating norm-conserving pseudopotentials with excellent transferability and employing an extremely efficient iterative diagonalization scheme optimized for our purpose. The self-consistent band structures, the total and site-projected densities of states, the partial charges and their symmetry-decompositions, and some characteristic charge densities near E_F are presented. We compare our results with various existing (F)LAPW and (F)LMTO calculations and establish that the *ab initio* pseudopotential method is competitive with other methods in studying the electronic structure of such complicated materials as high- T_c cuprates.

PACS numbers: 74.72.Bk, 74.25.Jb, 71.25.-s, 71.20.-b

Typeset using REVTeX

I. INTRODUCTION

The discovery of superconductivity above 30K in $\text{La}_{2-x}\text{Ba}_x\text{CuO}_4$ by Bednorz and Müller [1] has stimulated intensive studies on various cuprates as well as the mechanism underlying the phenomenon of high- T_c superconductivity. A wide variety of speculations about its microscopic origin have been raised with the sole consensus of the apparently important role of the CuO_2 layer (and, of course, the pairing of charge carriers) which is the basic building block of high- T_c cuprates. Even for the *normal* (above T_c) state of the high- T_c cuprates, the controversy as to whether it is a Fermi liquid or some other novel states has not been settled. The reason for the complication is that many of the cuprate superconductors have sister compounds which are strongly correlated insulating antiferromagnets. Among novel points of view explaining anomaly in normal states of high- T_c cuprates are the Luttinger liquid theory, the marginal Fermi liquid theory, the van Hove scenario, the spin fluctuation theory, the extended Hubbard model, the t - J model, and the anyon theory, to mention a few. On the other side of such efforts, there has been a more conventional approach dealing with the full Hamiltonian and the realistic atomic structure in the belief of the Fermi liquid theory; the first principles density functional theory [2] with the local density approximation (LDA) [3] for the exchange-correlation energy is such an example. In spite of its shortcomings in the magnetic insulating phase, the various state-of-the-art electronic structure calculations have proven to be successful in predicting from first principles a number of properties of metallic cuprates such as the lattice constant, atomic positions within the unit cell, phonon frequencies, structural instabilities, electric field gradients, and most importantly, the detailed energy band structure and the Fermi surface (FS) [4]. Such calculations show the existence of a half-filled $pd\sigma$ -antibonding band and the resulting cylindrical FS per CuO_2 plane as the distinctive electronic feature of the high- T_c cuprates [5].

Most of the existing electronic structures for high- T_c cuprates have been calculated with use of the all-electron localized basis methods (LMTO, FLMTO, LAPW, or FLAPW) or the pseudopotential mixed basis method. Here, we want to emphasize the merits of the plane-wave basis set, which above-mentioned methods do not share. The mathematical formulation and the implementation of the numerical codes are particularly simple with the plane-wave basis set. The accuracy of calculation is easily controlled by varying the

kinetic energy cutoff. Plane-waves form a basis set independent of the ionic positions, allowing for an unbiased uniform description of the system and a much simpler calculation of quantum mechanical (Hellman-Feynman) forces. Furthermore, plane waves enable us to use the fast Fourier transform so that the iterative diagonalization methods [6–10] or the *ab initio* molecular dynamics [11–13] can be applied efficiently. In conjunction with the pseudopotential formulation [14,15] where the rapid oscillations of valence wavefunctions in the core region are systematically smoothed out with their norms kept conserved, the plane-wave basis sets are quite successful in the calculation of the electronic structure of most semiconductors and some metals. However, until recently it was believed that materials including first-row elements, transition-metal atoms, and rare-earth elements are not suitable for the application of the pseudopotential plane-wave method. With the development of efficient methods for diagonalizing large Hamiltonian matrices represented in a plane-wave basis set [6–13], together with relatively smooth pseudopotentials [16,17], it is now possible to perform the electronic structure calculations for systems containing such atoms.

In this paper, we present an *ab initio* pseudopotential density-functional calculation of $\text{YBa}_2\text{Cu}_3\text{O}_7$ using the plane-wave basis set. $\text{YBa}_2\text{Cu}_3\text{O}_{7-\delta}$ ($0 \leq \delta \leq 1$) is perhaps the most extensively studied compound among the cuprate superconductors. A unique feature of this compound is that the three copper atoms in the primitive cell play two different roles. Two copper atoms (Cu2) participate in two conduction layers of CuO_2 separated by yttrium atoms. The third copper atom (Cu1) has an unusual coordination with oxygen atoms, forming a one-dimensional CuO chain structure along the b direction. The stoichiometric compound $\text{YBa}_2\text{Cu}_3\text{O}_7$ is particularly interesting from the standpoint of band theorists. It crystallizes in the relatively simple structure (with 13 atoms in the orthorhombic primitive cell) allowing for the computation with a less severe load compared with Bi- or Tl-based cuprate superconductors. More importantly, it is a metal instead of an anti-ferromagnetic insulator in its normal state in contrast to other stoichiometric cuprates like La_2CuO_4 . Aside from the problem in handling the strong correlation among electrons, the local density functional (LDF) calculation is applicable to this system. Furthermore, clean surfaces are available in this compound so that high resolution spectroscopic experiments can be performed and the theoretical results can be compared directly with experiments.

The quasiparticle band near the Fermi level and the FS topology from the ARPES [18], ACAR [19], and dHvA [20] experiments are in good accordance with those obtained from the existing LDF calculations [21–29]. This fact is sometimes regarded as supporting evidence for the Fermi liquid picture of the normal state of high- T_c cuprates though the issue is still controversial. Since the main purpose of the present work is to show the feasibility of the *ab initio* pseudopotential plane-wave method for studying high- T_c materials in comparison with other methods and since the present paper is the first such report to our knowledge, we will exhibit below a rather extensive amount of figures obtained through the fully-converged pseudopotential calculation, but avoid promoting a particular theory for the high- T_c superconducting mechanism.

II. COMPUTATIONAL METHOD

We generate soft norm-conserving pseudopotentials using the scheme of Troullier and Martins [16], which gives a very fast convergence of the total energy with respect to the basis-set size. (It is possible to use *ultrasoft* pseudopotentials [30] which require a much smaller basis set size at the price of abandoning the norm-conserving property, but we do not adopt that scheme here.) To enhance the transferability of the pseudopotential and guarantee correct scattering properties of the pseudopotential, we include some semi-core orbitals into the valence shell and use ionized configurations for the atoms Y and Ba. The configuration and the cutoff radii r_{cl} 's with which the pseudopotentials are generated are listed in Table I. All the pseudopotentials, except for the oxygen pseudopotential, are generated semi-relativistically. The partial core correction scheme [31] is employed to overcome the problem associated with the nonlinearity of the exchange-correlation functional. The Ceperly-Alder correlation [32] is used in the parametrized version of Perdew and Zunger [33]. These pseudopotentials are then cast into the fully-nonlocal separable form of Kleinman and Bylander [34] with use of *s*-locality to avoid the ghost states [35,36]. The norm-conserving requirement results in the matched first energy derivative of the logarithmic derivative of the wavefunction, $\frac{\partial}{\partial \epsilon} \frac{\partial}{\partial r} \log R_l(r)|_{\epsilon=\epsilon_l, r=r_{cl}}$, between the pseudo radial wavefunction and the all-electron one, where $R_l(r)$ and ϵ_l are the radial wavefunction and the valence orbital energy for angular momentum l . The pseudopotentials optimized by us with the above scheme

show scattering properties acceptable in a much wider energy range than enforced by the norm-conserving condition.

We then perform the plane-wave band structure calculations within the LDA. The single-particle Kohn-Sham equation is solved by diagonalizing the Hamiltonian matrix [37]. Diagonalization is achieved by using the block-Davidson method [6,7] with the modified Jacobi relaxation [8–10]. At this point, we want to mention the superiority of the block-Davidson method with the modified Jacobi relaxation to two other competing methods, the DIIS-*ritzit* [8–10] and the preconditioned conjugate gradient [12,13] methods, in dealing with systems with relatively localized states. We have tested these three diagonalization schemes by studying the cubic ZnS with variable submatrix sizes. For relatively small submatrix sizes, the block-Davidson method still gives correct results, whereas the latter two methods frequently fail to do it. The discrepancy is due to the fact that the block-Davidson method updates the eigenvectors simultaneously while the latter two adopt a band-by-band updating scheme. Actually, there exists a crossover behavior in relative merits among the three schemes. If the number of desired states is very large, the computational load in diagonalizing the Hamiltonian projected to the expansion space is too severe with the first method and the latter two methods with a sufficiently large submatrix is preferable to the first one. As the number decreases, however, the computational effort of the first method in the diagonalization of the expansion-space-projected Hamiltonian is greatly reduced and the block-Davidson method is superior to the other two.

III. RESULTS AND DISCUSSION

The calculation for the stoichiometric $\text{YBa}_2\text{Cu}_3\text{O}_7$ are performed with use of the recently obtained structural parameters at 10K [38]; $a = 3.8196\text{\AA}$, $b = 3.8813\text{\AA}$, $c = 11.64028\text{\AA}$, $z_{\text{Ba}} = 0.18388$, $z_{\text{Cu2}} = 0.35457$, $z_{\text{O2}} = 0.37823$, $z_{\text{O3}} = 0.37813$, and $z_{\text{O4}} = 0.15976$. The atomic positions in lattice unit are $\text{Y}(\frac{1}{2}, \frac{1}{2}, \frac{1}{2})$, $\text{Ba}(\frac{1}{2}, \frac{1}{2}, \pm z_{\text{Ba}})$, $\text{Cu1}(0, 0, 0)$, $\text{Cu2}(0, 0, \pm z_{\text{Cu2}})$, $\text{O1}(0, \frac{1}{2}, 0)$, $\text{O2}(\frac{1}{2}, 0, \pm z_{\text{O2}})$, $\text{O3}(0, \frac{1}{2}, \pm z_{\text{O3}})$, and $\text{O4}(0, 0, \pm z_{\text{O4}})$. The cutoff energy of 72.25 Ry and 147 \mathbf{k} -points in the irreducible Brillouin zone (IBZ, 1/8 of the Brillouin zone) with the linear tetrahedron method [39,40] are used to obtain the self-consistency. The self-consistent energy bands are plotted in Fig. 1 along the symmetry directions in the IBZ. The same band

structure is shown in expanded scale in Fig. 2 for the energy range from -1.0 eV to 3.0 eV. There are four partially filled bands crossing E_F . Two nearly half-filled bands are derived from the two CuO_2 planes and have the usual two-dimensional character of $\text{Cu}2(3d_{x^2-y^2})\text{--O}2(2p_x)\text{--O}3(2p_y)$ σ -antibonding. The other two are derived from the CuO chain and show negligible dispersions along S-Y and R-T in contrast to appreciable dispersions along X-S and U-R. The two CuO chain bands show completely different bonding characters. The nearly-empty dispersive band has the character of $\text{Cu}1(3d_{yz})\text{--O}1(2p_y)\text{--O}4(2p_z)$ σ -antibonding and the almost filled flat band has the $\text{Cu}1(3d_{yz})\text{--O}1(2p_z)\text{--O}4(2p_y)$ π -antibonding character. Four E_F -crossing bands form a complicated FS's shown in Fig. 3; one stick, two cylinders along the c direction, and one sheet perpendicular to the Γ -Y direction. There are many published literatures presenting either the energy band structure or the FS's of $\text{YBa}_2\text{Cu}_3\text{O}_7$, all of which resort to localized basis methods. Among them, the first report was made by Yu *et al.* [21,22] and illustrates an overall feature of the band structure of $\text{YBa}_2\text{Cu}_3\text{O}_7$, but shows a somewhat unconverged result — the existence of a hole-like cylindrical FS along Y-T. Later Massidda [24] assigned the incorrectness to the small number (10) of \mathbf{k} -points and corrected it with use of a larger number (32) of \mathbf{k} -points. The second report by Krakauer *et al.* [23] shows more converged results than Yu *et al.*, but the interaction between plane bands and the chain band are incorrectly described as will be discussed below. Results of the subsequent calculation by the same group (Pickett *et al.* [25]) are different from its preceding work; the band-band interaction is correctly described but the chain derived band along Γ -Y, which is slightly unfilled in Krakauer *et al.* [23], lies below E_F . Andersen *et al.*'s FLMT0 results [27] are indistinguishable from Pickett *et al.*'s. There is a calculation done by using the pseudopotential mixed-basis method [28], but the resulting energy bands show poor convergence. Judging from the band structure and the calculated FS's, the present pseudopotential plane-wave calculation shows the most converged results with accuracy comparable with Pickett *et al.* [25] and Andersen *et al.* [27]. (Though the FS topology is different for the large plane-derived band, it is fragile with respect to the variation of E_F on a scale as small as ~ 0.01 eV.) The present results are also in good agreement with experiments [18–20].

The bonding nature of the four partially filled bands can be clarified by examining their

charge density contour plots at some selected \mathbf{k} -points. The charge densities of the states at $\mathbf{k} = (\frac{1}{4}, \frac{1}{4}, 0)$, a half way from Γ to S, for the lower and the upper CuO₂ bands are shown in Figs. 4(a) and (b) respectively. Both of them reflect the Cu2($d_{x^2-y^2}$)-O2(p_x)-O3(p_y) σ -antibonding hybridization characteristic of the high- T_c cuprates. In detail, however, their symmetries are different. The wavefunction of the lower CuO₂ band is the symmetric linear combination of the two CuO₂ plane states residing above and below the Y atom plane, and the upper CuO₂ band is the antisymmetric one, which can be deduced from the comparison of the smallest-value contour lines in Figs. 4(a) and (b). Furthermore, their parity with respect to the chain plane reflection is even for the lower band and odd for the upper one, respectively. Since the wavefunctions of the nearly-empty chain band are even with respect to the reflection in the plane of the chains perpendicular to c axis, it follows that for $k_z = 0$ the chain band does cross the odd (upper) plane band while hybridizing with the even (lower) plane band. For $k_z = \frac{\pi}{c}$, the situation is reversed, *i.e.*, the nearly-empty chain band interacts with the upper plane band but does not with the lower one. Such symmetry properties and the interaction between the plane bands and the nearly-empty chain band are mentioned in Pickett *et al.* [25] and fully described in Mazin *et al.* [29].

The charge densities of the nearly-empty chain band are shown in Fig. 5 at $\mathbf{k} = (\frac{1}{2}, \frac{1}{2}, 0)$ and $(\frac{1}{4}, \frac{1}{4}, 0)$. The Cu1($d_{y^2-z^2}$)-O1(p_y)-O4(p_z) σ -antibonding character and the local four-fold coordination of the Cu1 atom are clearly identified from them. The absence of the band dispersion along S-Y or R-T can be ascribed to the strong one-dimensional character along the b axis. As the energy rises towards the S point the antibonding character of the Cu1-O1 bond increases while that of Cu1-O4 is almost unaffected. The shorter Cu1-O4 bond length of 1.8596Å compared with the Cu2-O4 interatomic distance of 2.2676Å is consistent with the bonding characters identified above. The Cu1-O1-O4 $pd\sigma$ -antibonding band is almost empty, while its bonding counterpart is completely filled. It is therefore likely for O4 atoms to be tightly bonded to Cu1 atoms. On the other hand, the Cu2 atoms have no ligand O atom on the Y plane side. The Cu2($d_{3z^2-r^2}$) orbitals are only weakly bonded to O4 and both the bonding and antibonding bands are almost filled, resulting in a weaker Cu2-O4 bond and a longer Cu2-O4 interatomic distance.

The contour plots of the charge density for the fourth (almost filled) band are shown in

Fig. 6 at $\mathbf{k} = (\frac{1}{2}, \frac{1}{2}, 0)$ and $(\frac{1}{4}, \frac{1}{4}, 0)$. A remarkable feature is that the main contribution to this band comes from $O1(p_z)$ and $O4(p_y)$ orbitals and relatively little charge resides at the Cu, O2, and O3 atoms. The character at S is $O1(p_z)$ – $O4(p_y)$ – $Cu1(d_{yz})$ – $Cu2(d_{yz})$ π -antibonding and the charge is depleted on the zx -plane. The states near $\mathbf{k} = (\frac{1}{4}, \frac{1}{4}, 0)$ have the $O1(p_z)$, $O4(p_x, p_y, p_z)$, $Cu1(d_{yz}, d_{zx})$, $Cu2(d_{z^2-x^2})$, and $O2(p_z)$ orbital characters. Since these chain-related states lie in the narrow energy region containing E_F , they are expected to be strongly affected as the oxygen content on the CuO chain is reduced and the hole doping concentration decreases, implying that T_c should be influenced significantly by these states.

The muffin-tin radii of 2.80, 3.20, 1.95, and 1.65 a.u. for Y, Ba, Cu, and O atoms respectively are used in calculating the partial charges and the partial (or site-projected and symmetry-decomposed) densities of states (PDOS). The total density of states (TDOS) at E_F is 1.41 states/(eV Cu). For comparison, Massidda *et al.* [21] obtained $N(E_F)$ = 1.13 states/(eV Cu) and Krakauer *et al.* [23] 1.38. The PDOS plots in Fig. 7 show that the Cu1–O1–O4 sates prevail in the energy range from 0.5 eV below E_F to E_F . The PDOS in an expanded scale in Fig. 8 indicates a van Hove singularity at ~ 0.03 eV below E_F with a clear Cu1–O1–O4 hybridization. The importance of the van Hove singularity to the high- T_c mechanism has been strongly advocated in some theoretical studies [41]. The partial charges and their symmetry decompositions are listed in Table II. (The partial charges and their symmetry decompositions are presented and fully analyzed in Schwarz *et al.* [26].) The relatively small amount of $O1(p_y)$, $O4(p_z)$, $Cu1(d_{x^2-y^2})$, and $Cu1(d_{3z^2-r^2})$ partial charges are due to the nearly-empty dispersive band of $Cu1(d_{y^2-z^2})$ – $O1(p_y)$ – $O4(p_z)$ hybridization. In fact, with use of a different choice of symmetry decomposition including $d_{y^2-z^2}$ symmetry, the partial charge of $Cu1(d_{y^2-z^2})$ is further reduced to 1.30, which is smaller than the partial charge of $Cu1(d_{3z^2-r^2})$, 1.38. The relatively small amount of $O2(p_x)$, $O3(p_y)$, and $Cu2(d_{x^2-y^2})$ partial charges compared with the other $O2(p)$, $O3(p)$, and $Cu2(d)$ partial charges is attributed to the characteristic $pd\sigma$ -antibonding hybridization [$Cu2(d_{x^2-y^2})$ – $O2(p_x)$ – $O3(p_y)$] of the superconducting cuprates. The smaller partial charge of $Cu1(3d_{y^2-z^2})$ than that of $Cu2(3d_{x^2-y^2})$ (1.30 versus 1.42) is in accordance with the existence of the nearly-empty chain band and two nearly half-filled plane bands. The partial

charges of the Cu($4p$) states are relatively small, but their magnitude can serve as a measure of the bond strength between a copper atom and its neighboring atoms. The Cu($4p$) partial charges do not originate from *on-site* Cu($4p$) states, which lie at much higher energies, but represent the intrusion of wavefunctions centered at neighboring (off-site) atoms into the copper muffin-tin sphere. They originate mainly from the surrounding O($2p$) wavefunctions and their magnitude depends on the distance from copper to the neighboring oxygen sites. Since the Cu1–O4 bond length is shorter than that of Cu1–O1, the partial charge of Cu1(p_z) is larger than that of Cu1(p_y). The Cu1(p_x) partial charge is the smallest due to the absence of the oxygen neighbors in the a direction. For the plane copper atoms, the longer distance to O4 than to O2 or O3 manifests itself in the smaller Cu2(p_z) partial charge than that of Cu2(p_x) or Cu2(p_y).

IV. SUMMARY

We have applied, for the first time, the *ab initio* pseudopotential plane-wave method to the electronic structure calculation of the high- T_c cuprate YBa₂Cu₃O₇ within the LDF formalism. Soft pseudopotentials of optimized transferability are generated through the Troullier-Martins scheme and cast into the Kleinman-Bylander type fully-separable form. The block-Davidson algorithm with the modified Jacobi relaxation operator is then used to solve the single-particle Kohn-Sham equation. The energy bands, the Fermi surfaces, the charge densities, the total DOS, the partial DOS, and the symmetry-decomposed partial charges obtained here are in good agreement with both the existing theoretical calculations using (F)LMTO and (F)LAPW methods and the available experimental facts. This successful application to YBa₂Cu₃O₇ has demonstrated that one can deal with systems containing first row elements, transition metals, or rare-earth elements with acceptable computational efforts via the *ab initio* pseudopotential plane-wave method.

Helpful discussions with Prof. Jaejun Yu are greatly appreciated. This work is supported by the Ministry of Science and Technology, the '94 Basic Science Research Program of the Ministry of Education, the SNU Daewoo Research Fund, and the Korea Science and Engineering Foundation through the SRC program.

REFERENCES

- [1] J. G. Bednorz and K. A. Müller, Z. Phys. B **64**, 189 (1986).
- [2] P. Hohenberg and W. Kohn, Phys. Rev. **136**, B864 (1964).
- [3] W. Kohn and L. J. Sham, Phys. Rev. **140**, A1133 (1965).
- [4] There is a review paper which provides a collection of the local-density functional calculations on high- T_c cuprates until 1988. See W. E. Pickett, Rev. Mod. Phys. **61**, 433 (1989).
- [5] Recently an *ad hoc* half-filled σ -antibonding band criterion for identifying possible high- T_c candidates is suggested. See L. F. Mattheiss, Phys. Rev. B **47**, 8224 (1993).
- [6] E. R. Davidson, J. Comput. Phys. **17**, 87 (1975).
- [7] B. Liu, in *Report on the Workshop ‘Numerical Algorithms in Chemistry: Algebraic Methods’ of the National Resource for Computation in Chemistry*, edited by C. Moler and I. Shavitt (Lawrence Berkeley Lab., Univ. of California, 9–11 August 1978), p 49.
- [8] D. M. Wood and A. Zunger, J. Phys. A **18**, 1343 (1985).
- [9] J. L. Martins and M. L. Cohen, Phys. Rev. B **37**, 6134 (1988).
- [10] J. L. Martins and N. Troullier, Phys. Rev. B **43**, 2213 (1991).
- [11] R. Car and M. Parrinello, Phys. Rev. Lett. **55**, 2471 (1985).
- [12] M. P. Teter, M. C. Payne and D. C. Allan, Phys. Rev. B **40**, 12255 (1989).
- [13] M. C. Payne, M. P. Teter, D. C. Allan, T. A. Arias, and J. D. Joannopoulos, Rev. Mod. Phys. **64**, 1045 (1992).
- [14] D. R. Hamann, M. Schlüter, and C. Chiang, Phys. Rev. Lett. **43**, 1494 (1979).
- [15] G. B. Bachelet, D. R. Hamann, and M. Schlüter, Phys. Rev. B **26**, 4199 (1982).
- [16] N. Troullier and J. L. Martins, Phys. Rev. B **43**, 1993 (1991).
- [17] A. M. Rappe, K. M. Rabe, E. Kaxiras, and J. D. Joannopoulos, Phys. Rev. B **41**, 1227

- (1990).
- [18] J. C. Kampuzano, G. Jennings, M. Faiz, L. Beaulaigue, B. W. Veal, J. Z. Liu, A. P. Paulikas, K. Vandervoort, H. Claus, R. S. List, A.J. Arko, and R. J. Bartlett, Phys. Rev. Lett. **64**, 2308 (1990); G. Mante, R. Claessen, R. Manzke, M. Skibowski, Th. Wolf, M. Knupfer, and J. Fink, Phys. Rev. B **44**, 9500 (1991); R. Liu, B. W. Veal, A. P. Paulikas, J. W. Downey, P. J. Kostić, S. Fleshler, U. Welp, C. G. Olson, X. Wu, A. J. Arko, and J. J. Joyce, Phys. Rev. B **46**, 11056 (1992).
 - [19] H. Haghighi, J. H. Kaiser, S. Rayner, R. N. West, J. Z. Liu, R. Shelton, R. H. Howell, F. Solal, and M. J. Fluss, Phys. Rev. Lett. **67**, 382 (1991).
 - [20] C. M. Fowler, B. L. Freeman, W. L. Hults, J. C. King, F. M. Mueller, and J. L. Smith, Phys. Rev. Lett. **68**, 534 (1992).
 - [21] S. Massidda, J. Yu, A. J. Freeman, and D. D. Koeling, Phys. Lett. A **122**, 198 (1987).
 - [22] J. Yu, S. Massidda, A. J. Freeman, and D. D. Koeling, Phys. Lett. A **122**, 203 (1987).
 - [23] H. Krakauer, W. E. Pickett, and R. E. Cohen, J. Supercond. **1**, 111 (1988).
 - [24] S. Massidda, Physica C **169**, 137 (1990).
 - [25] W. E. Pickett, R. E. Cohen, and H. Krakauer, Phys. Rev. B **42**, 8764 (1990).
 - [26] K. Schwarz, C. Ambrosch-Draxl, and P. Blaha, Phys. Rev. B **42**, 2051 (1990).
 - [27] O. K. Andersen, A. I. Liechtenstein, O. Rodriguez, I. I. Mazin, O. Jepsen, V. P. Antropov, O. Gunnarsson, and S. Gopalan, Physica C **185-189**, 147 (1991).
 - [28] M. Hiroi, T. Uda, and Y. Murayama, Physica C **185-189**, 1551 (1991).
 - [29] I. I. Mazin, S. N. Rashkeev, A. I. Liechtenstein, and O. K. Andersen, Phys. Rev. B **46**, 11232 (1992).
 - [30] D. Vanderbilt, Phys. Rev. B **41**, 7892 (1990).
 - [31] S. G. Louie, S. Froyen, and M. L. Cohen, Phys. Rev. B **26**, 1738 (1982).
 - [32] D. M. Ceperly and B. J. Alder, Phys. Rev. Lett. **45**, 566 (1980).

- [33] J. P. Perdew and A. Zunger, Phys. Rev. B **23**, 5048 (1981).
- [34] L. Kleinman and D. M. Bylander, Phys. Rev. Lett. **48**, 1425 (1982).
- [35] X. Gonze, P. Käckel, and M. Scheffler, Phys. Rev. B **41**, 12264 (1990).
- [36] X. Gonze, R. Stumpf, and M. Scheffler, Phys. Rev. B **44**, 4238 (1991).
- [37] J. Ihm, A. Zunger, and M. L. Cohen, J. Phys. C **12**, 4409 (1979) and J. Phys. C **13**, 3095 (1980).
- [38] R. P. Sharma, F. J. Rotella, J. D. Jorgensen, and L. E. Rehn, Physica C **174**, 409 (1991).
- [39] G. Lehmann and M. Taut, Phys. Status Solidi (b) **54**, 469 (1972).
- [40] J. Rath and A. J. Freeman, Phys. Rev. B **11**, 2109 (1975).
- [41] C. C. Tsuei, D. M. Newns, C. C. Chi, and P. C. Pattnaik, Phys. Rev. Lett. **65**, 2724 (1990).

TABLES

TABLE I. The reference configurations and core radii. For Y and Ba atoms, +3 and +2 ionized configurations are used respectively to get optimal pseudopotentials.

atom	Y	Ba	Cu	O
configuration	$4s^2 4p^6 4d^1$	$5s^2 5p^6 5d^0$	$4s^1 4p^0 3d^{10}$	$2s^2 2p^4$
r_{cs}	1.19	1.65	2.06	1.15
r_{cp}	1.35	2.00	2.30	1.45
r_{cd}	2.49	2.48	2.06	-

TABLE II. The symmetry-decomposed partial charges (in electrons) of the valence states of $\text{YBa}_2\text{Cu}_3\text{O}_7$.

atom	s	x	y	z	p	xy	yz	zx	$x^2 - y^2$	$3z^2 - r^2$	d	total
Y	0.086	0.069	0.066	0.070	0.204	0.048	0.136	0.146	0.137	0.052	0.521	0.811
Ba	0.062	0.135	0.123	0.120	0.377	0.092	0.039	0.058	0.037	0.060	0.286	0.725
Cu1	0.194	0.028	0.059	0.079	0.167	1.836	1.856	1.837	1.644	1.379	8.552	8.912
Cu2	0.175	0.063	0.059	0.033	0.156	1.848	1.811	1.809	1.419	1.738	8.627	8.957
O1	0.039	1.238	0.984	1.300	3.522	0.003	0.003	0.000	0.003	0.001	0.009	3.570
O2	0.043	1.068	1.287	1.251	3.606	0.003	0.000	0.003	0.004	0.001	0.011	3.660
O3	0.042	1.285	1.064	1.252	3.600	0.003	0.003	0.000	0.003	0.001	0.010	3.652
O4	0.041	1.228	1.258	1.041	3.527	0.000	0.002	0.002	0.000	0.004	0.008	3.576

Figure Captions

FIG. 1. The energy band structure of $\text{YBa}_2\text{Cu}_3\text{O}_7$.

FIG. 2. The energy band structure of $\text{YBa}_2\text{Cu}_3\text{O}_7$ on (a) $k_z = 0$ plane and (b) $k_z = \frac{\pi}{c}$ plane in expanded scale. The inset in (b) is the band structure in much more expanded scale illustrating the band crossing between the chain band and the lower plane band as well as the band repulsion between the chain band and the upper plane band.

FIG. 3. The FS's of $\text{YBa}_2\text{Cu}_3\text{O}_7$ derived from the four partially filled bands. The solid line is the stick-like FS along S-R from the almost filled chain band, the short-dashed line indicates the one-dimensional FS arising from the nearly-empty chain band, the long-dashed line is the cylindrical FS from the upper CuO_2 band, and the medium-dashed line from the lower CuO_2 band.

FIG. 4. The charge density contours of $\text{YBa}_2\text{Cu}_3\text{O}_7$ for states at $\mathbf{k} = (\frac{1}{4}, \frac{1}{4}, 0)$ of (a) the lower Cu2–O2–O3 plane band and (b) the upper Cu2–O2–O3 plane band. Contour values run from 0.0002 to 0.0102 in steps of 0.002 e/unit-cell. The symbols \bullet and \blacklozenge represent Cu and O atoms respectively.

FIG. 5. The charge density contours of $\text{YBa}_2\text{Cu}_3\text{O}_7$ for the nearly-empty Cu1–O1–O4 σ -antibonding chain band at (a) $\mathbf{k} = (\frac{1}{2}, \frac{1}{2}, 0)$ and (b) $\mathbf{k} = (\frac{1}{4}, \frac{1}{4}, 0)$. Contour values run from 0.001 to 0.011 in steps of 0.002 e/unit-cell.

FIG. 6. The charge density plots of the almost filled chain-related band of $\text{YBa}_2\text{Cu}_3\text{O}_7$ at (a) $\mathbf{k} = (\frac{1}{2}, \frac{1}{2}, 0)$ and (b) $\mathbf{k} = (\frac{1}{4}, \frac{1}{4}, 0)$. Contour values are the same as in Fig. 5.

FIG. 7. The total and the partial densities of states of $\text{YBa}_2\text{Cu}_3\text{O}_7$. (a) The TDOS, (b) the PDOS of chain-related atoms, and (c) the PDOS of plane-related atoms.

FIG. 8. (a) The TDOS, (b) the PDOS of chain-related atoms, and (c) the PDOS of plane-related atoms of $\text{YBa}_2\text{Cu}_3\text{O}_7$ near E_F in expanded scale.

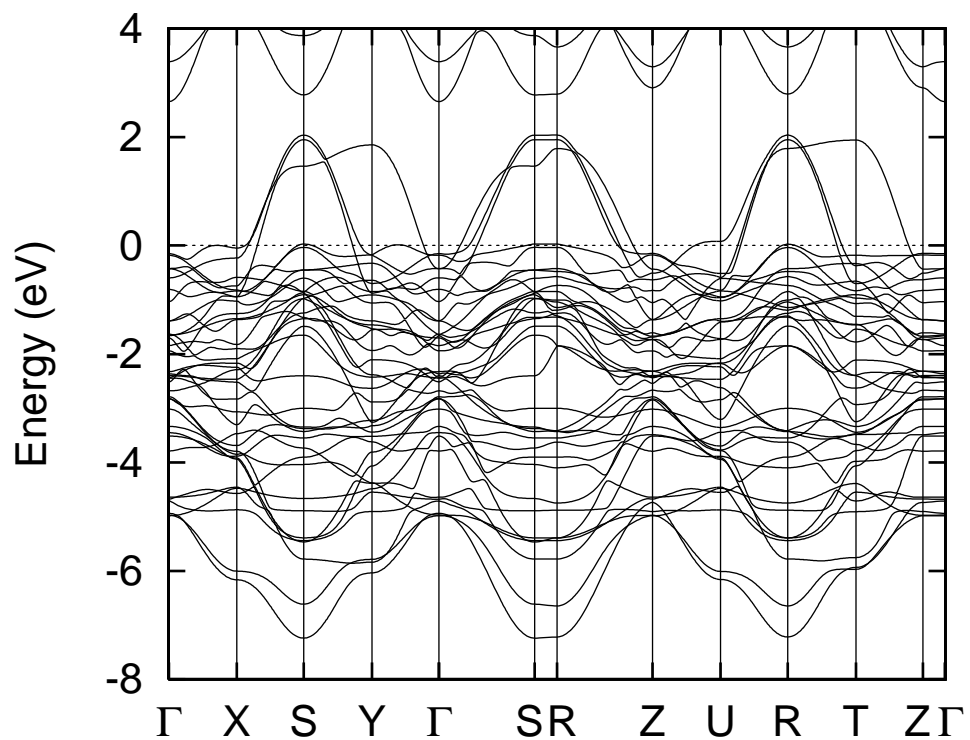


Fig. 1

*Hanchul Kim et al. "Ab initio Pseudopotential ..."
submitted to Phys. Rev. B1*

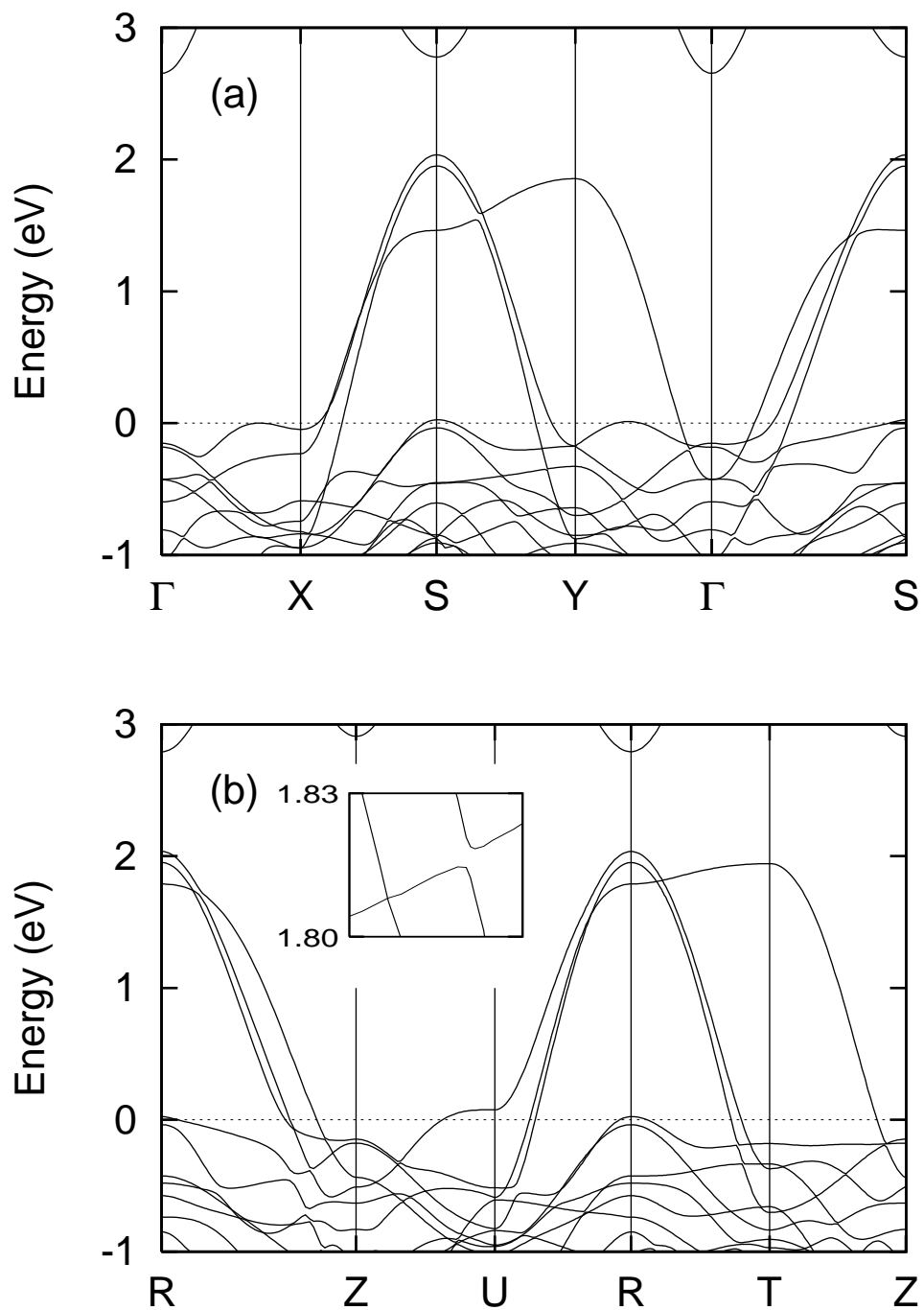


Fig. 2

Hanchul Kim et al. "Ab initio Pseudopotential ..."
submitted to Phys. Rev. B1

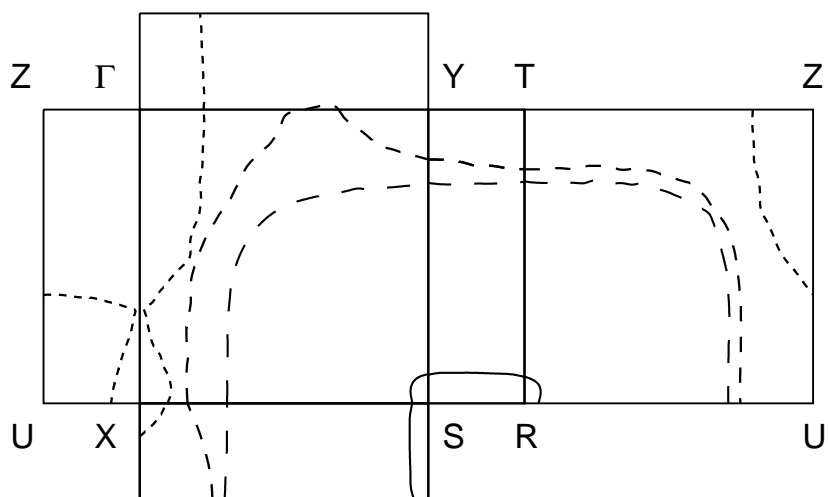


Fig. 3

*Hanchul Kim et al. "Ab initio Pseudopotential ..."
submitted to Phys. Rev. B1*

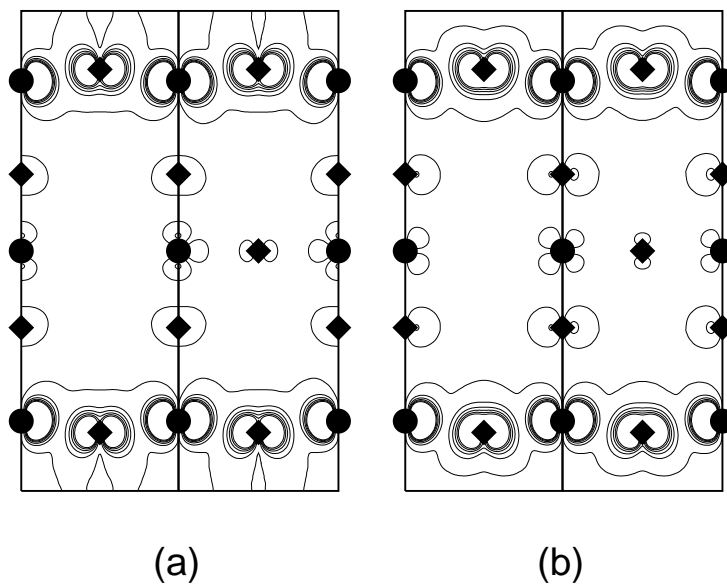


Fig. 4

Hanchul Kim et al. "Ab initio Pseudopotential ..."
submitted to Phys. Rev. B1

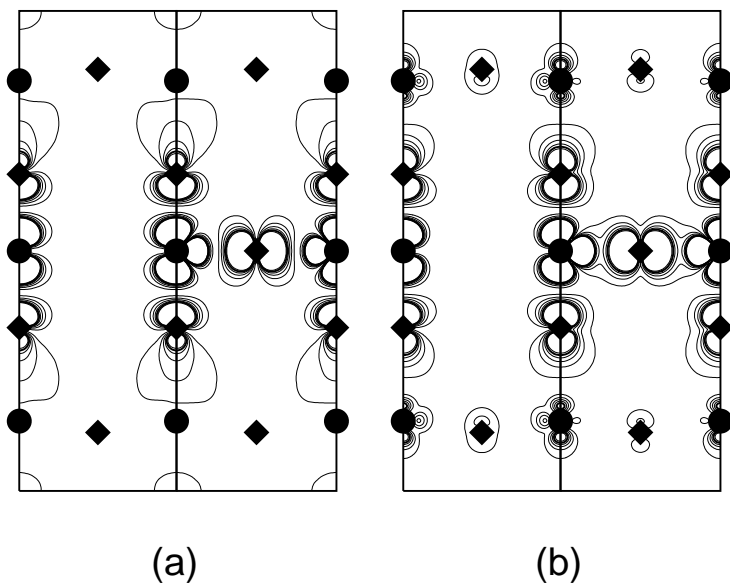


Fig. 5

*Hanchul Kim et al. "Ab initio Pseudopotential ..."
submitted to Phys. Rev. B1*

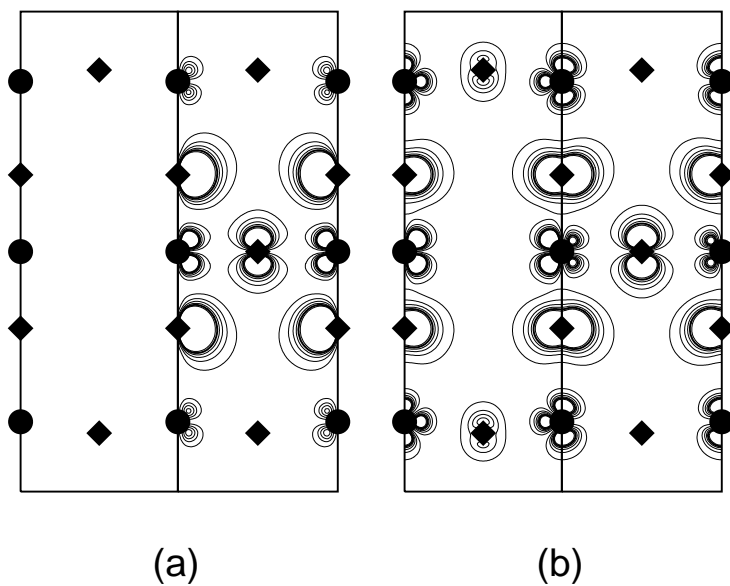


Fig. 6

*Hanchul Kim et al. "Ab initio Pseudopotential ..."
submitted to Phys. Rev. B1*

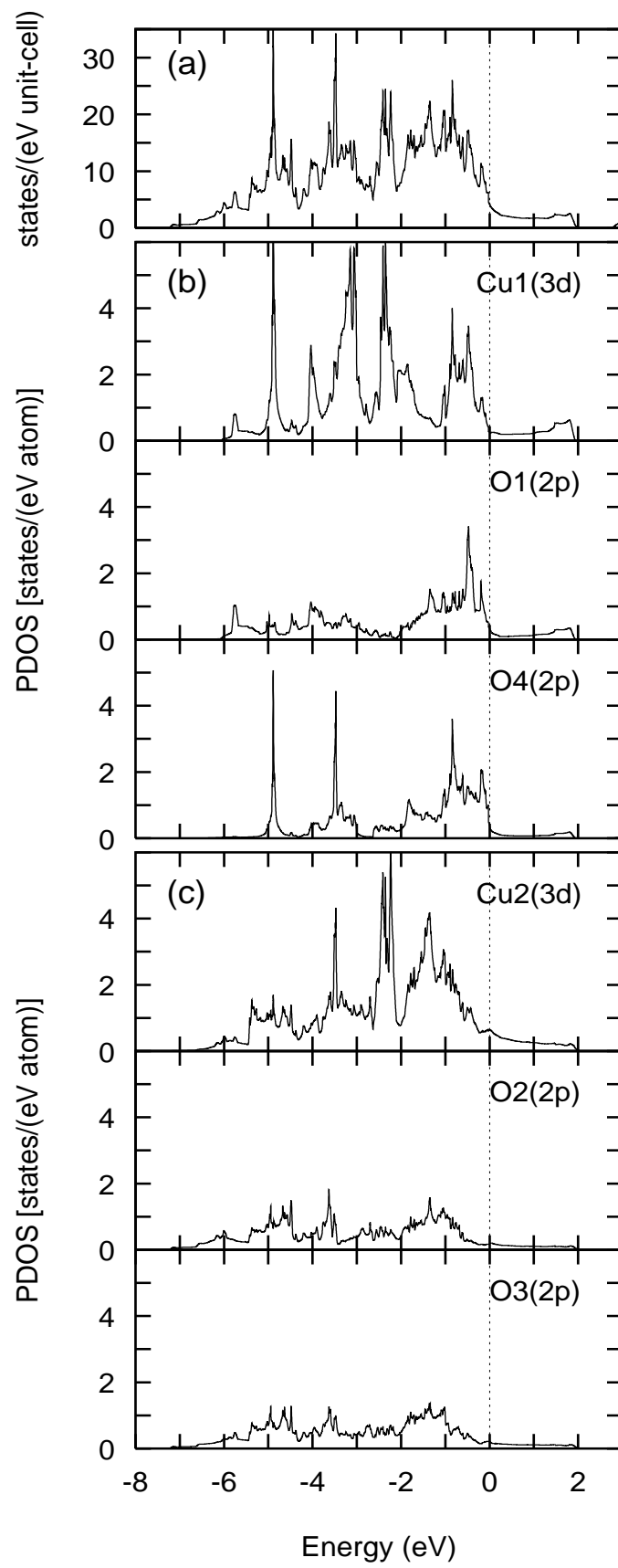


Fig. 7

Hanchul Kim et al. "Ab initio Pseudopotential ..."
submitted to Phys. Rev. B1

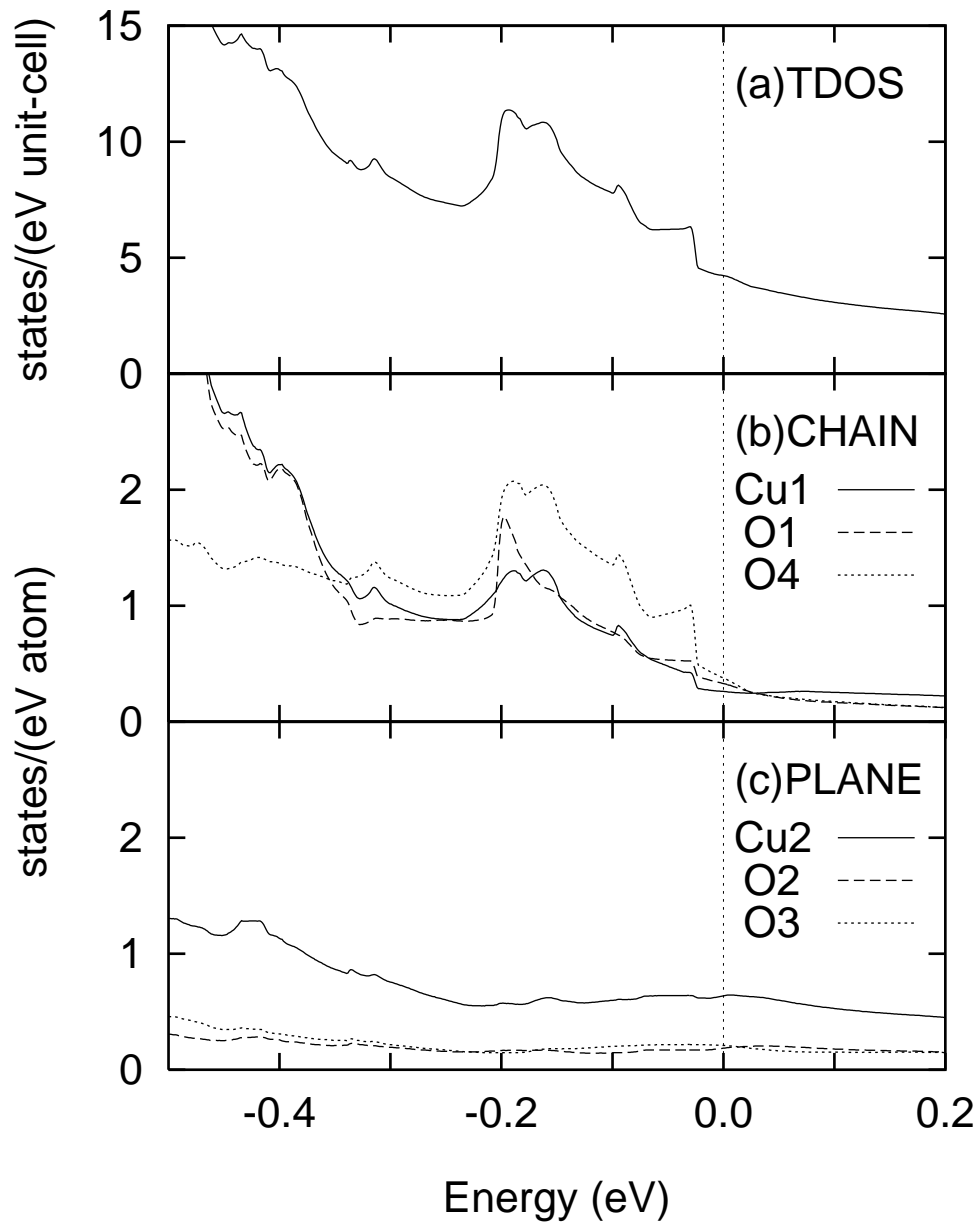


Fig. 8

Hanchul Kim et al. "Ab initio Pseudopotential ..."
submitted to Phys. Rev. B1